Universal Faraday Rotation in HgTe Wells with Critical Thickness

A. Shuvaev,[1] V. Dziom,[1] Z. D. Kvon,[2,3] N. N. Mikhailov,[2,3] and A. Pimenov[1]
[1]*Institute of Solid State Physics, Vienna University of Technology, 1040 Vienna, Austria*
[2]*Novosibirsk State University, Novosibirsk 630090, Russia*
[3]*Institute of Semiconductor Physics, Novosibirsk 630090, Russia*
(Received 3 April 2016; published 6 September 2016)

The universal value of the Faraday rotation angle close to the fine structure constant ($\alpha \approx 1/137$) is experimentally observed in thin HgTe quantum wells with a thickness on the border between trivial insulating and the topologically nontrivial Dirac phases. The quantized value of the Faraday angle remains robust in the broad range of magnetic fields and gate voltages. Dynamic Hall conductivity of the holelike carriers extracted from the analysis of the transmission data shows a theoretically predicted universal value of $\sigma_{xy} = e^2/h$, which is consistent with the doubly degenerate Dirac state. On shifting the Fermi level by the gate voltage, the effective sign of the charge carriers changes from positive (holes) to negative (electrons). The electronlike part of the dynamic response does not show quantum plateaus and is well described within the classical Drude model.

DOI: 10.1103/PhysRevLett.117.117401

The strong spin-orbit coupling and an inverted band structure in mercury telluride makes this material a nearly universal tool to probe novel physical effects, with the film thickness being a tuning parameter [1,2]. If the thickness of HgTe wells is below critical, $d < d_c \approx 6.3$ nm, the sequence of the conduction and valence bands is conventional and a trivial insulating state is realized. For thicker films and in the bulk mercury telluride, the inversion of valence and conduction bands leads to topologically nontrivial surface states [3,4]. This state is characterized by the locking of the electron spin and the electron momentum, and they are topologically protected against nonmagnetic impurity scattering.

If the HgTe well exhibits critical thickness, the gap between the valence and conduction bands disappears and a two-dimensional (2D) electron gas is formed with a Dirac cone dispersion [1,2]. Close to the center of the Dirac cone, the electron spin is not a good quantum number but has to be replaced by pseudospin or helicity [3,5]. Because of the particle-hole symmetry of these states, the quantum Hall effect shifts by a half integer and takes the form $\sigma_{xy} = \gamma(n + 1/2)e^2/h$. In the well-investigated case of graphene [6,7], the states are fourfold degenerate, i.e., $\gamma = 4$, as two Dirac cones are present in the Brillouin zone which are both doubly spin degenerate.

Magneto-optics in the terahertz range has proven to be an effective tool for investigating two-dimensional conducting states in several quantum systems, such as graphene [8–10], Bi_2Se_3 [11–14], and HgTe [15–22]. Magneto-optical spectroscopy has the advantages of being contact free and of directly accessing the effective mass m_c via the cyclotron resonance $\Omega_c = eB/m_c$. Here, B is the external magnetic field.

In the dynamical regime, the unusual character of the quantum Hall effect in systems with Dirac cones can be shown [23–26] to lead to universal values for the Faraday and Kerr rotations of $\theta_F = \alpha \sim 1/137$ and $\theta_K = \pi/2$, respectively. Such predictions have recently been confirmed experimentally in graphene [9], where the Faraday angle is additionally doubled, as two Dirac cones exist in the Brillouin zone. Very recently [27–29], several groups announced the observation of the quantized Faraday and Kerr rotations from the surface states of various topological insulators. In our previous work [29], the universal Faraday rotation was observed on surface states in a three-dimensional topological insulator, realized in thick strained HgTe film.

Compared to thick strained films with 3D carriers, in HgTe wells with critical thickness, a two-dimensional electron gas is realized. In this case there is no gap between the valence and conduction bands, resulting in Dirac dispersion of the 2D carriers. Because of the double degeneracy of the Dirac cone, the quantized dynamical Hall conductivity with $\gamma = 2$ may be expected.

In this Letter we present the results of the terahertz experiments in HgTe quantum wells with critical thickness. Compared to graphene [9], here a single valley Dirac fermion system is realized revealing strong spin-orbit coupling. Critical sample thickness ensures a 2D character of charge carriers which can be tuned using a transparent gate.

Mercury telluride quantum wells have been grown on (013) oriented GaAs substrates by molecular beam epitaxy, as described elsewhere [30]. The results on two samples with thickness close to critical are presented: sample 1 with $d = 6.3$ nm and sample 2 with $d = 6.6$ nm. The gate on both samples has been prepared *ex situ* using a mylar film with $d = 6$ μm as an insulating barrier and a semitransparent metallized film as a gate (Ti, $R = 600$ $\Omega/\square$). In the

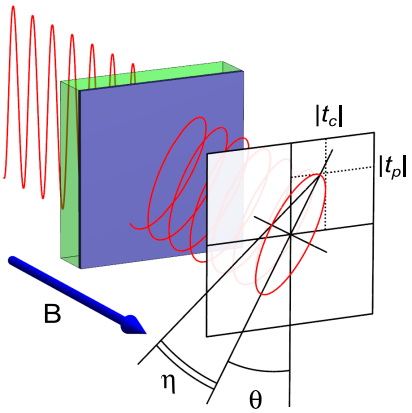

FIG. 1. Schematic view of the magneto-optical experiment to measure the Faraday rotation θ and ellipticity η. The definitions of both angles are depicted in the output polarization ellipse, assuming linear incident polarization. The external magnetic field is applied in the Faraday geometry, i.e., $B\|\mathbf{k}$. Complex transmission in parallel (t_p) and crossed (t_c) polarizers are measured, which provides a full description of the transmission matrix.

experiment, the gate conductivity is seen as a magnetic field-independent and frequency independent contribution to σ_{xx}. No measurable effect of the gate on Hall conductivity has been observed, which agrees well with the low mobility of the gate carriers.

The experimental results in this Letter have been obtained using a Mach-Zehnder interferometer operating at submillimeter wavelengths (0.1–1 THz) [31]. The interferometric arrangement has enabled us to obtain the absolute values of complex transmissions through the sample in parallel and crossed polarizer geometries [32]. The experimental procedure is shown schematically in Fig. 1. External magnetic fields up to 7 T have been applied using a superconducting magnet with polypropylene windows. The transmission experiments have been done in the Faraday geometry; i.e., a magnetic field is applied along the propagation direction of the electromagnetic radiation. In total, four experimental parameters are measured, and a full characterization of the transmitted radiation is obtained including the polarization state. With this information, the Faraday rotation angle θ and the ellipticity η can be obtained directly [19,32,33].

Explicit equations for calculating the matrix of the conductivity from the measured transmission are given in Ref. [33]. In these calculations the effect of the GaAs substrate and of Ti gate are taken into account exactly; i.e., pure HgTe conductivity is obtained. The measured Faraday rotation and ellipticity are still partly influenced by the properties of the substrate and the gate. Where appropriate, specific values of these angles will be given. The frequency of the transmission experiment is chosen to minimize the influence of the substrate.

The most important result of this Letter is demonstrated in Fig. 2. Here, the experimental Faraday rotation θ (the

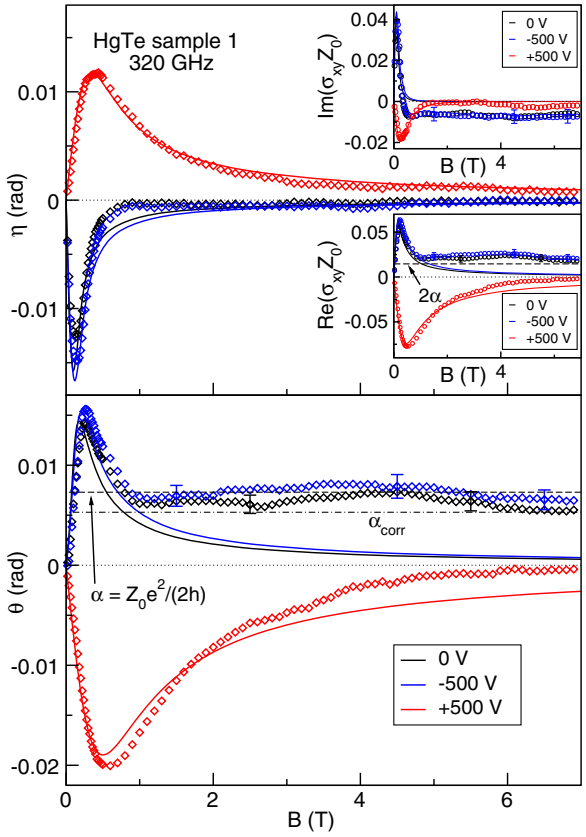

FIG. 2. Magnetic field dependence of the Faraday rotation θ (lower panel) and ellipticity η (upper panel) for sample 1 for three characteristic gate voltages. Experimental data are shown by solid symbols and the lines are fits within the Drude model [26,34]. The dashed line shows a "pure" universal value of the Faraday rotation $\alpha \approx 1/137$ rad. The dash-dotted line gives the real value of the rotation α_{corr}, taking into account the influence of the substrate and gate and assuming $\sigma_{xy} = e^2/h$. (Inset) The off-diagonal conductivity σ_{xy} as directly obtained from the spectra using exact expressions for the magneto-optical transmission [33].

lower panel) and ellipticity η (the upper panel) are shown for sample 1. The peaks in the data at around $B \sim 0.5$ T are the cyclotron resonances on free charge carriers in our sample. The sign change of the Faraday angle and the ellipticity between the negative and positive gate voltages corresponds to the transition from the holelike to the electronlike carrier, respectively.

We note that, in high magnetic fields far above the cyclotron resonance [35], classical Faraday rotation and ellipticity are expected to fade out, as $\theta \sim 1/B$, $\eta \sim 1/B^2$. Remarkably, in Fig. 2 the experimental values of the Faraday rotation for zero and negative gate voltages saturate at fields above 1 T and stay constant within the experimental accuracy up to the highest field in our experiment (7 T). We note that similar broad steps in the quantum Hall resistivity have recently been observed in HgTe wells and attributed to heavy hole valley reservoir

effects [36]. The step in Faraday rotation reveals a universal value close to the fine structure constant $\alpha = (Z_0/2)(e^2/h)$, indicated in Fig. 2 by dashed lines. The dash-dotted line gives a value which takes into account the properties of the substrate and gate precisely [33] and assumes $\sigma_{xy} = e^2/h$, $\sigma_{xx} = 0$. The difference between both values of Faraday rotation and the experimental data are within the uncertainties of the present work. As discussed above, in HgTe with critical thickness, a 2D electron gas with Dirac dispersion is realized with double degeneracy [1,2]. Therefore, we attribute the observation of $\theta \approx \alpha$ to doubly degenerate states, each contributing by $\alpha/2$.

In order to demonstrate the discrepancy between the experimental data and classical cyclotron resonance, the fits within the Drude model [26,34] are shown as solid lines in Fig. 2. The Faraday rotation θ and the Faraday ellipticity η of the electronlike carriers at positive gate voltage are well fitted within the classical response (the red lines and symbols). The ellipticity at zero and the negative gate voltages also follow the classical Drude model quite well. Remarkably, the experimental Faraday rotation in this region of the gate voltages behaves very distinctly from the predictions of the model. The model curves tend towards zero rather quickly at fields above 1 T (the blue and black lines). To the contrary, the experimental data show an abrupt deviation from the classical calculations at these fields, saturating at an approximately constant level.

From the transmission spectra in a zero magnetic field and at zero gate voltage, the exact value of the refractive index of the substrate (the optical thickness) is determined experimentally [32]. With this parameter, the transmission in both parallel and crossed geometries can be recalculated into the complex magneto-optical conductivity of mercury telluride [33] without additional assumptions. The diagonal conductivity σ_{xx} is mostly responsible for the parallel transmission in our experiments and for the dissipation in dc transport measurements. The off-diagonal conductivity σ_{xy} is related to the transmission in the crossed geometry and for the quantum Hall plateaus in the dc experiments. σ_{xy} is especially relevant for the emergence of the universal Faraday rotation α; it is plotted in the inset of Fig. 2. The data are shown in a dimensionless form by multiplying the conductivity σ with the impedance of vacuum $Z_0 \approx 377\ \Omega$.

The upper inset in Fig. 2 shows the imaginary part of σ_{xy}, which appears at nonzero frequencies only. The real part of σ_{xy} is shown in the lower inset. It also demonstrates the deviation from the classical Drude behavior and saturates at the level slightly above the universal value of $Z_0(e^2/h) = 2\alpha$. We attribute this deviation to the uncertainties of the experiment.

From the Drude fits of the dynamic conducivity of sample 1 in the vicinity of the cyclotron resonance, the parameters of the charge carriers could be calculated and are given in Table I. Much lower mobility of the electrons (+500 V) compared to holes (−500 V) is probably the reason that no quantized Faraday effect could be observed for positive voltages. High Dirac-hole mobility in HgTe wells can be explained by a screening of their scattering by heavy holes [37].

TABLE I. Drude parameters of the charge carriers in HgTe sample 1 as obtained from the fits of magneto-optical conductivity: density n_{2D}, effective mass m_c/m_0, and mobility μ. The gate voltage −500 V corresponds to hole carriers and +500 V to electrons, respectively. m_0 is the free electron mass.

Gate (V)	n_{2D} (cm^{-2})	m_c/m_0	μ (cm^2/V · s)
−500 V	$(3.3\pm0.5)\times10^{10}$	$(7.5\pm1)\times10^{-3}$	$(6.6\pm1.0)\times10^{4}$
+500 V	$(1.4\pm0.3)\times10^{11}$	$(9.2\pm1)\times10^{-3}$	$(2.0\pm0.2)\times10^{4}$

At a fixed frequency of the incident radiation $f =$ 320 GHz and at $T = 1.8$ K, there are two external parameters which can be tuned: the magnetic field and the gate voltage. A good overview of the experimental data set obtained by changing both parameters is provided by Fig. 3. Here, the color coded height represents the Faraday rotation θ as a function of the magnetic field $-2\ \text{T} < B < 2\ \text{T}$ and of the gate voltage $-500\ \text{V} < U <$ 500 V in the direction of increasing voltage. The data shown in Fig. 2 are cuts of the parametric surface in Fig. 3 at fixed gate voltages. The cyclotron resonance peaks in Fig. 2 are also seen in Fig. 3. However, now it is possible to see the continuous evolution of the cyclotron resonances with the gate voltage. The positive peak at positive magnetic fields and the gate voltage of −500 V gradually disappears and transforms into a negative peak at +500 V. This is a manifestation of the transition from the holelike carriers at negative gate voltages to the electronlike carriers at the positive gates.

The main result of this Letter, a plateau in Faraday rotation close to the universal value $\theta = \alpha$, is supported by the measurements on sample 2. Eight contacts have been prepared around the edges of sample 2, which allowed us to measure the dc longitudinal and transverse resistivities R_{xx} and R_{xy}. These data are shown in the upper inset of Fig. 4. The black curve is the longitudinal resistivity R_{xx}, while the red curve represents the transverse resistivity R_{xy}. The pronounced plateau at the fields between 0.75 and 1.5 T is clearly seen in the R_{xy} data. The value of the transverse resistivity at the plateau is around 25.8 kΩ, which could be expected if only the last quantum Hall plateau were observed and the degeneracy factor were equal to $\gamma = 2$. The dc data correspond well to the universal value of the Faraday rotation $\theta = \alpha$. Indeed, in the limit of small absorption by thin film [35], we may write $\theta \sim t_c/t_p \sim t_c \sim Z_0/2R_{xy}$, which leads to $\theta = \alpha$ for $R_{xy} = h/e^2$. Direct correspondence between the quantum Hall effect and quantized Faraday rotation is well known in ordinary 2D electron gases [38].

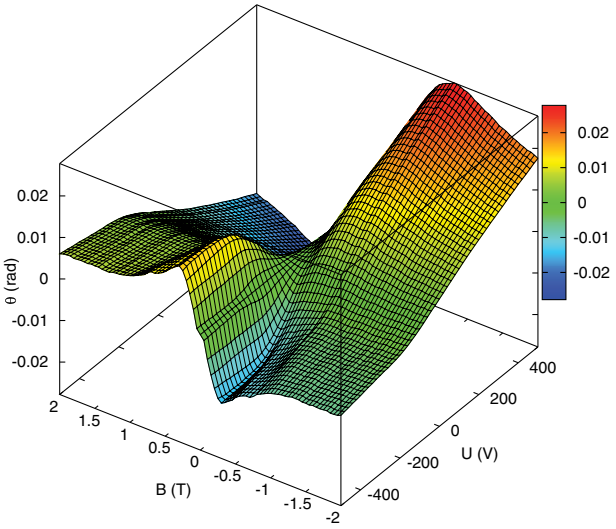

FIG. 3. Faraday rotation θ of HgTe quantum well no. 1 as a function of gate voltage and the magnetic field. The values of θ are color coded for clarity. The data are given for the increasing gate voltage from -500 V to $+500$ V as applied to the gate electrode. The maximum and minimum of θ at low magnetic fields are the manifestations of the cyclotron resonance. The inversion from maximum to minimum reflects the transition from the holelike charge carriers at negative gate voltages to the electronlike charge carriers at positive voltages.

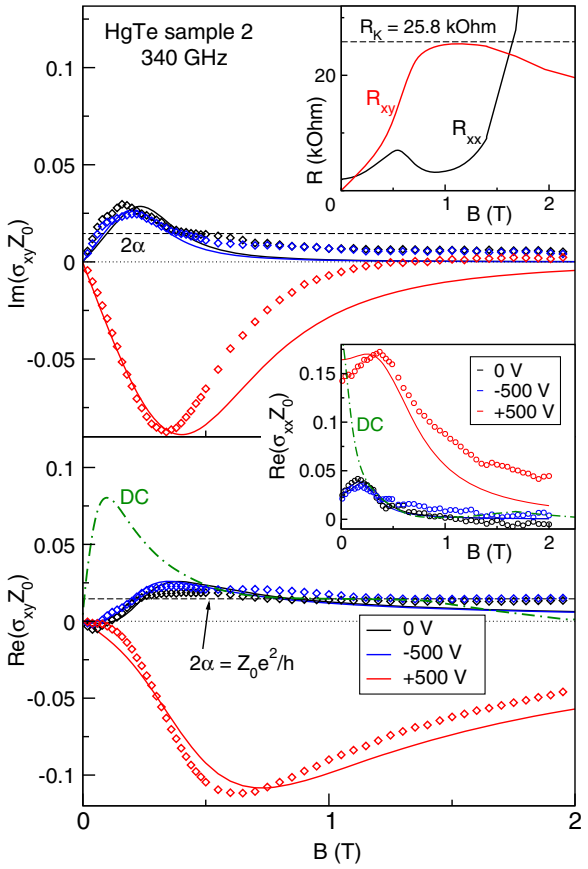

FIG. 4. Magnetic field dependence of the off-diagonal conductivity σ_{xy} for sample 2 at different gate voltages. The symbols represent experimental data, while the lines are fits using the Drude model. The green dash-dotted line shows the conductivity calculated from the dc data. Black dashed lines show the universal value of conductivity (2α) predicted for doubly degenerate Dirac fermions. (Upper inset) dc longitudinal and Hall resistivity measured on the same sample. The divergence of R_{xx} in high magnetic fields is due to a field-induced transition to the insulating state. (Lower inset) The diagonal dynamic conductivity σ_{xx}, with the Drude fit and dc data represented as solid and dash-dotted lines, respectively. The maximum in σ_{xx} close to 0.2 T corresponds to the cyclotron resonance.

The magneto-optical conductivity of sample 2 is shown in Fig. 4. The imaginary part in the upper panel reveals no plateau at either the positive or the negative gate voltage. The real part of the conductivity shown in the lower panel demonstrates a clear plateau at fields above 1 T at zero and negative gate voltages. The value of this plateau is equal to $\sigma_{xy}Z_0 = 2\alpha = Z_0 e^2/h$, and it corresponds well to the dc data shown by a green line. In the electronlike doping regime at the positive gate voltage, no such plateau is observed in magnetic fields below 2 T.

An interesting difference between the dc and the THz conductivity of HgTe films is that the high frequency measurements show the robust plateau in the Faraday rotation θ up to 2 T in Fig. 4 and up to 7 T in Fig. 2, whereas in the dc data the plateau is limited to the field range ~0.8–1.3 T. In addition, R_{xx} reveals a clear indication of insulating behavior above 1.5 T. This could be due to the quantum Hall liquid-to-insulator transition [39–41]. In the static experiment, the current has to follow the percolation path across the whole sample and the liquid-to-insulator transition sets in rather quickly. To the contrary, at high frequencies the charge carriers are able to move a small distance only $[\ell \sim \min(v_F\tau, v_F/\nu) \sim 1\ \mu\text{m}]$ during one period of the electromagnetic wave. Here [19], $v_F \sim 10^6$ m/s is the Fermi velocity, $\tau \sim 10^{-12}$ s is the scattering time, and ν is the frequency of the experiment. The less conducting regions of the sample are not participating in the overall response while the signal from the conducting parts is still present. Therefore, one can expect that the transition to an insulating state will disappear at high frequencies, as observed here.

In conclusion, using polarization- and phase-sensitive terahertz transmission spectroscopy, HgTe quantum wells with critical thickness are investigated. In external magnetic fields, a universal value of the Faraday rotation close to the fine structure constant $\theta_F = \alpha \approx 1/137$ is observed for holelike carriers. Dynamic Hall conductivity is directly calculated from the experiment, and it reveals a universal value $\sigma_{xy} = e^2/h$ which corresponds to a degeneracy $\gamma = 2$ of the Dirac states. The universal steps in the dynamical conductivity and the Faraday angle remain robust in a broad range of external magnetic fields and gate voltages.

On the electronic side of the gate voltages, a classical magneto-optical behavior is observed. It can be attributed to the much lower mobility of negatively charged carriers.

We thank G. Tkachov, E. M. Hankiewicz, and S.-C. Zhang for the valuable discussions. This work was supported by the Austrian Science Fund (Grants No. I815-N16, No. W-1243, and No. P27098-N27).

[1] B. A. Bernevig, T. L. Hughes, and S.-C. Zhang, Science **314**, 1757 (2006).
[2] B. Büttner, C. X. Liu, G. Tkachov, E. G. Novik, C. Brüne, H. Buhmann, E. M. Hankiewicz, P. Recher, B. Trauzettel, S. C. Zhang *et al.*, Nat. Phys. **7**, 418 (2011).
[3] X.-L. Qi, T. L. Hughes, and S.-C. Zhang, Phys. Rev. B **78**, 195424 (2008).
[4] M. Z. Hasan and C. L. Kane, Rev. Mod. Phys. **82**, 3045 (2010).
[5] A. H. Castro Neto, F. Guinea, N. M. R. Peres, K. S. Novoselov, and A. K. Geim, Rev. Mod. Phys. **81**, 109 (2009).
[6] K. S. Novoselov, A. K. Geim, S. V. Morozov, D. Jiang, M. I. Katsnelson, I. V. Grigorieva, S. V. Dubonos, and A. A. Firsov, Nature (London) **438**, 197 (2005).
[7] Y. Zhang, Y. Tan, H. Stormer, and P. Kim, Nature (London) **438**, 201 (2005).
[8] I. Crassee, J. Levallois, A. L. Walter, M. Ostler, A. Bostwick, E. Rotenberg, T. Seyller, D. van der Marel, and A. B. Kuzmenko, Nat. Phys. **7**, 48 (2011).
[9] R. Shimano, G. Yumoto, J. Y. Yoo, R. Matsunaga, S. Tanabe, H. Hibino, T. Morimoto, and H. Aoki, Nat. Commun. **4**, 1841 (2013).
[10] M. Orlita, I. Crassee, C. Faugeras, A. B. Kuzmenko, F. Fromm, M. Ostler, T. Seyller, G. Martinez, M. Polini, and M. Potemski, New J. Phys. **14**, 095008 (2012).
[11] A. A. Schafgans, K. W. Post, A. A. Taskin, Y. Ando, X.-L. Qi, B. C. Chapler, and D. N. Basov, Phys. Rev. B **85**, 195440 (2012).
[12] S. Bordács, J. G. Checkelsky, H. Murakawa, H. Y. Hwang, and Y. Tokura, Phys. Rev. Lett. **111**, 166403 (2013).
[13] L. Wu, M. Brahlek, R. V. Aguilar, A. V. Stier, C. M. Morris, Y. Lubashevsky, L. S. Bilbro, N. Bansal, S. Oh, and N. P. Armitage, Nat. Phys. **9**, 410 (2013).
[14] P. Olbrich, L. E. Golub, T. Herrmann, S. N. Danilov, H. Plank, V. V. Bel'kov, G. Mussler, C. Weyrich, C. M. Schneider, J. Kampmeier *et al.*, Phys. Rev. Lett. **113**, 096601 (2014).
[15] A. M. Shuvaev, G. V. Astakhov, A. Pimenov, C. Brüne, H. Buhmann, and L. W. Molenkamp, Phys. Rev. Lett. **106**, 107404 (2011).
[16] J. N. Hancock, J. L. M. van Mechelen, A. B. Kuzmenko, D. van der Marel, C. Brüne, E. G. Novik, G. V. Astakhov, H. Buhmann, and L. W. Molenkamp, Phys. Rev. Lett. **107**, 136803 (2011).
[17] Z. D. Kvon, S. N. Danilov, D. A. Kozlov, C. Zoth, N. N. Mikhailov, S. A. Dvoretskii, and S. D. Ganichev, JETP Lett. **94**, 816 (2012).
[18] M. Zholudev, F. Teppe, M. Orlita, C. Consejo, J. Torres, N. Dyakonova, M. Czapkiewicz, J. Wróbel, G. Grabecki, N. Mikhailov *et al.*, Phys. Rev. B **86**, 205420 (2012).
[19] A. M. Shuvaev, G. V. Astakhov, G. Tkachov, C. Brüne, H. Buhmann, L. W. Molenkamp, and A. Pimenov, Phys. Rev. B **87**, 121104 (2013).
[20] P. Olbrich, C. Zoth, P. Vierling, K.-M. Dantscher, G. V. Budkin, S. A. Tarasenko, V. V. Bel'kov, D. A. Kozlov, Z. D. Kvon, N. N. Mikhailov *et al.*, Phys. Rev. B **87**, 235439 (2013).
[21] C. Zoth, P. Olbrich, P. Vierling, K.-M. Dantscher, V. V. Bel'kov, M. A. Semina, M. M. Glazov, L. E. Golub, D. A. Kozlov, Z. D. Kvon *et al.*, Phys. Rev. B **90**, 205415 (2014).
[22] K.-M. Dantscher, D. A. Kozlov, P. Olbrich, C. Zoth, P. Faltermeier, M. Lindner, G. V. Budkin, S. A. Tarasenko, V. V. Bel'kov, Z. D. Kvon *et al.*, Phys. Rev. B **92**, 165314 (2015).
[23] W.-K. Tse and A. H. MacDonald, Phys. Rev. B **82**, 161104 (2010).
[24] J. Maciejko, X.-L. Qi, H. D. Drew, and S.-C. Zhang, Phys. Rev. Lett. **105**, 166803 (2010).
[25] W.-K. Tse and A. H. MacDonald, Phys. Rev. Lett. **105**, 057401 (2010).
[26] G. Tkachov and E. M. Hankiewicz, Phys. Rev. B **84**, 035405 (2011).
[27] K. N. Okada, Y. Takahashi, M. Mogi, R. Yoshimi, A. Tsukazaki, K. S. Takahashi, N. Ogawa, M. Kawasaki, and Y. Tokura, Nat. Commun. **7**, 12245 (2016).
[28] L. Wu, M. Salehi, N. Koirala, J. Moon, S. Oh, and N. P. Armitage, arXiv:1603.04317.
[29] V. Dziom, A. M. Shuvaev, G. V. Astakhov, G. Tkachov, C. Brüne, H. Buhmann, L. W. Molenkamp, A. Pimenov, and E. M. Hankiewicz, arXiv:1603.05482.
[30] Z. D. Kvon, E. B. Olshanetsky, N. N. Mikhailov, and D. A. Kozlov, Low Temp. Phys. **35**, 6 (2009).
[31] A. A. Volkov, Y. G. Goncharov, G. V. Kozlov, S. P. Lebedev, and A. M. Prokhorov, Infrared Phys. **25**, 369 (1985).
[32] A. M. Shuvaev, G. V. Astakhov, C. Brüne, H. Buhmann, L. W. Molenkamp, and A. Pimenov, Semicond. Sci. Technol. **27**, 124004 (2012).
[33] V. Dziom, A. Shuvaev, N. N. Mikhailov, and A. Pimenov, arXiv:1603.05926.
[34] W.-K. Tse and A. H. MacDonald, Phys. Rev. B **84**, 205327 (2011).
[35] A. Shuvaev, A. Pimenov, G. V. Astakhov, M. Muhlbauer, C. Brune, H. Buhmann, and L. W. Molenkamp, Appl. Phys. Lett. **102**, 241902 (2013).
[36] D. A. Kozlov, Z. D. Kvon, N. N. Mikhailov, and S. A. Dvoretskii, JETP Lett. **100**, 724 (2015).
[37] D. A. Kozlov, Z. D. Kvon, N. N. Mikhailov, and S. A. Dvoretsky, JETP Lett. **96**, 730 (2013).
[38] V. A. Volkov and S. Mikhailov, JETP Lett. **41**, 476 (1985).
[39] T. Wang, K. P. Clark, G. F. Spencer, A. M. Mack, and W. P. Kirk, Phys. Rev. Lett. **72**, 709 (1994).
[40] H. W. Jiang, C. E. Johnson, K. L. Wang, and S. T. Hannahs, Phys. Rev. Lett. **71**, 1439 (1993).
[41] D. Shahar, D. C. Tsui, M. Shayegan, R. N. Bhatt, and J. E. Cunningham, Phys. Rev. Lett. **74**, 4511 (1995).